Supporting Information

Linkage Isomerism in a Homoleptic Fe(II) Complex with BODIPY-1*H*-Tetrazole Ligands

Matthias Schöbinger,[+*][a] Martin Huber,[+][a] Berthold Stöger,[b] and Peter Weinberger*[a]

[a]

Dr. M. Huber, Dr. M. Schöbinger, Prof. P. Weinberger
Institute of Applied Synthetic Chemistry, TU Wien
Getreidemarkt 9, 1060, Vienna (Austria)
E-mail: matthias.schoebinger@tuwien.ac.at, peter.e163.weinberger@tuwien.ac.at

[b]

Dr. B. Stöger
X-ray Center, TU Wien
Getreidemarkt 9/164, 1060, Vienna (Austria)

[+]

These authors contributed equally to this manuscript.

Table of Contents

Experimental protocols

All syntheses were performed with dried glassware, anhydrous and degassed solvents, and under an atmosphere of argon. Reaction monitoring was performed by IR-spectroscopy and XRPD. The ligand **L** (4,4-difluoro-1,3,5,7-tetramethyl-8- [(1H-tetrazol-1-yl)methyl]-4-bora-3a,4a-diaza-s-indacene) was synthesized according to a literature protocol,[1] all other starting materials were commercially purchased and used without further purifications if not stated otherwise.

Synthesis of coordination compounds 1 and 2

$Fe(ClO_4)_2 \cdot 6H_2O$ (9.16 mg, 0.0252 mmol, 1.00 equiv.) and a spatula tip of ascorbic acid were mixed in RCN (1 mL; R=$ClCH_2$ for **1**, R=$BrCH_2$ for **2**), filtrated and added to a mixture of **L** (50.0 mg, 0.151 mmol, 6.00 equiv.) and RCN (2 mL; R=$ClCH_2$ for **1**, R=$BrCH_2$ for **2**). After the reaction mixture was stirred at 40 °C overnight, it was cooled to room temperature and approx. 90 % of the solvent was evaporated, whereupon the formation of a precipitate could be reported. Diethyl ether (8 mL) was added to facilitate the precipitation of the crude product. The crude product was separated from the supernatant, washed with diethyl ether (3 x 6 mL) and dried in high vacuum to yield 42.4 mg (75.3 %) for **1**, 38.7 mg (68.9 %) for **2** as dark red solid.

Synthesis of coordination compounds 3 and 4a

$Fe(ClO_4)_2 \cdot 6H_2O$ (13.7 mg, 0.0379 mmol, 1.00 equiv.) and a spatula tip of ascorbic acid were mixed in solvent (1.5 mL; solvent = acetone for **3** and CH_3OH **4**), filtrated and added to a mixture of **L** (50.0 mg, 0.151 mmol, 4.00 equiv.) and again solvent (1.5 mL). After the reaction mixture was stirred at 40 °C overnight, it was cooled to room temperature and approx. 90 % of the solvent was evaporated, whereupon the formation of a precipitate could be reported. Diethyl ether (8 mL) was added to facilitate the precipitation of the crude product. The crude product was separated from the supernatant, washed with diethyl ether (3 x 6 mL) and dried in high vacuum to yield 36.2 mg (56.6 %) for **3** and 25.9 mg (41.7 %) for **4a** as dark red solid.

X-Ray Structure Determination

X-ray diffraction data of **1**, **2**, **3**, **4a** and **4b** (CSD 2463767–2463772) were collected at T = 100 K. and additionally T = 300 K for **1**, in a dry stream of nitrogen on a STOE STADIVARI diffractometer system equipped with a Dectris Eiger CdTe hybrid photon counting detector using either Cu-Kα (λ = 1.54186 Å) (**1**, **2**, **3**, **4a**) or Mo-Kα (λ = 0.71073 Å) (**4b**) radiation. Data were reduced with X-Area (X-Area 1.31.194.0, LANA 2.8.4; STOE & Cie GmbH, Darmstadt, Germany, 2024). An absorption correction was applied with the multi-scan approach implemented in LANA. The structures were solved by the dual-space approach implemented in SHELXT[3] and refined against F^2 with SHELXL.[4]

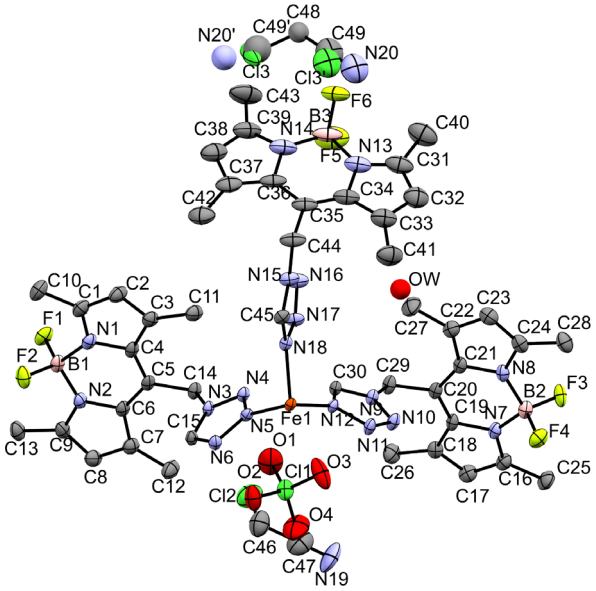

Figure S 1. Asymmetric unit of coordination compound **1** with atomic number labeling, showing the three different conformers of **L** (ellipsoids: 50 % probability level; atom color code: pink…B, grey…C, blue…N, red…O, light green…F, green…Cl, orange…Fe; H-atoms are omitted for clarity).

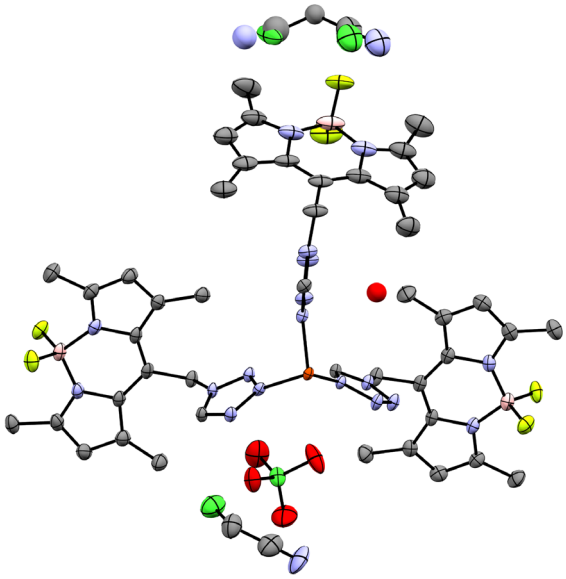

Figure S 2. Asymmetric unit of coordination compound **1**, showing the positions of the non-coordinating anion, the solvate molecules and the linkage isomerism of **L** (ellipsoids: 50 % probability level; atom color code: pink…B, grey…C, blue…N, red…O, light green…F, green…Cl, orange…Fe; H-atoms are omitted for clarity).

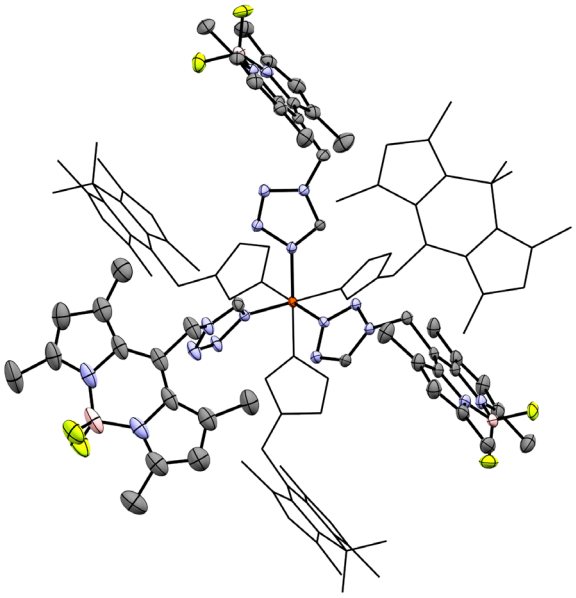

Figure S 3. Molecular structure of the homoleptic mononuclear complex of coordination compound **1** at 100 K, exhibiting the linkage isomerism of **L**; *N3* coordination mode of **L** in the equatorial plane front right and back left (ellipsoids: 50 % probability level; atom color code: pink…B, grey…C, blue…N, light green…F, orange…Fe; H-atoms, solvate molecules and non-coordinating anions are omitted for clarity; **L** molecules are partly depicted as wireframes for better visualization).

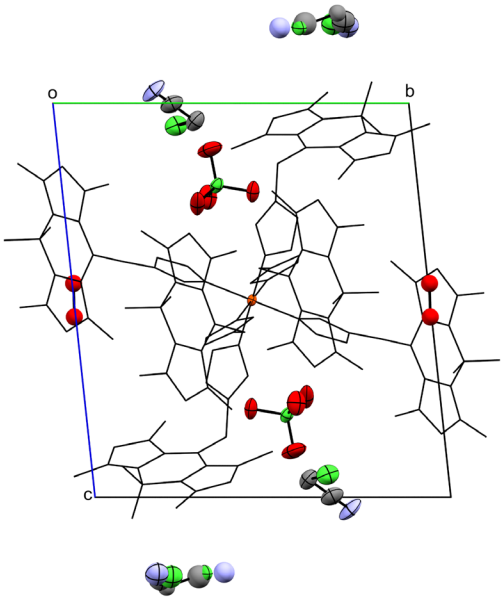

Figure S 4. Structure of coordination compound **1** at 100 K viewed along the crystallographic *a*-axis, showing the relative positions of the solvate molecules ($ClCH_2CN$ and H_2O) and the anion molecules (ClO_4^-) (ellipsoids: 50 % probability level; atom color code: pink…B, grey…C, blue…N, red…O, light green…F, green…Cl, orange…Fe; H-atoms are omitted for clarity and **L** molecules are depicted as wireframes for better visualization).

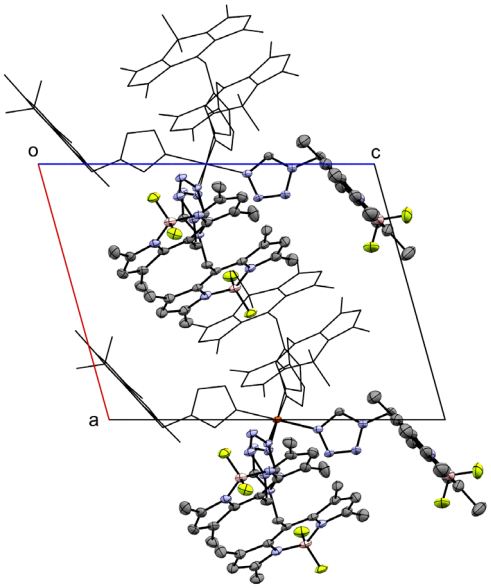

Figure S 5. Crystal packing of coordination compound **1** at 100 K, viewed along the crystallographic *b*-axis (ellipsoids: 50 % probability level; atom color code: pink…B, grey…C, blue…N, light green…F, orange…Fe; H-atoms, solvate molecules and non-coordinating anions are omitted for clarity; **L** molecules are depicted as wireframes for better visualization).

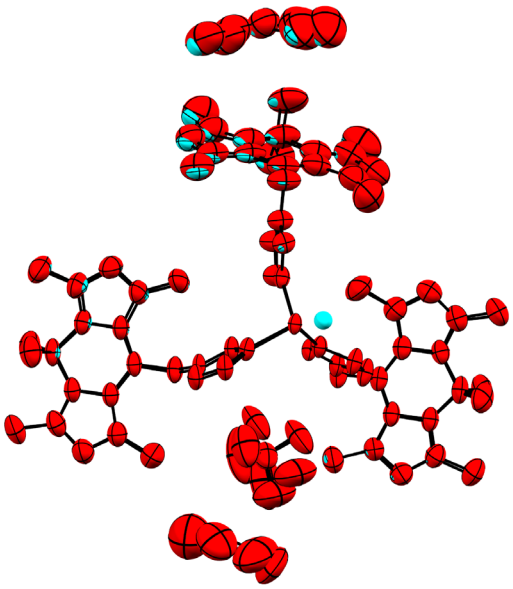

Figure S 6. Structure comparison of the asymmetric unit of coordination compound **1** at 100 K (cyan) and 300 K (red), showing differences in the incorporated solvate molecules (ellipsoids: 50 % probability level; H-atoms are omitted for clarity).

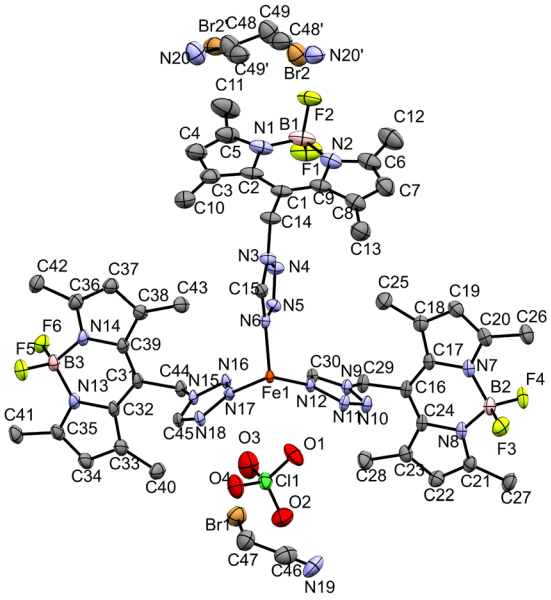

Figure S 7. Asymmetric unit of coordination compound **2** with atomic number labeling, showing the three different conformers of **L** (ellipsoids: 50 % probability level; atom color code: pink…B, grey…C, blue…N, red…O, light green…F, green…Cl, light bronze…Br, orange…Fe; H-atoms are omitted for clarity).

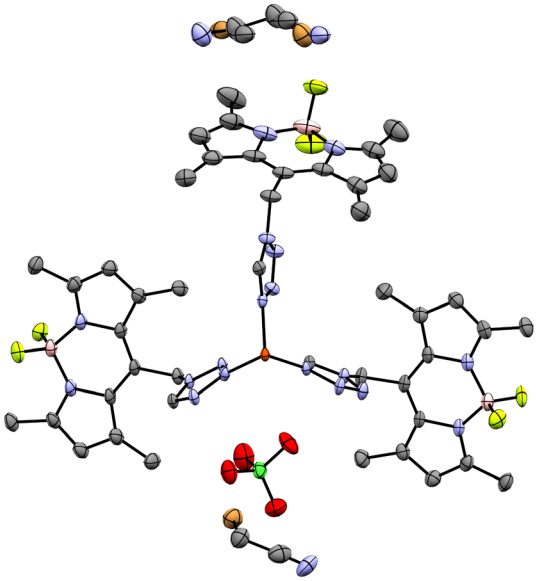

Figure S 8. Asymmetric unit of coordination compound **2**, showing the positions of the non-coordinating anion, the solvate molecules and the linkage isomerism of **L** (ellipsoids: 50 % probability level; atom color code: pink…B, grey…C, blue…N, red…O, light green…F, green…Cl, light bronze…Br, orange…Fe; H-atoms are omitted for clarity).

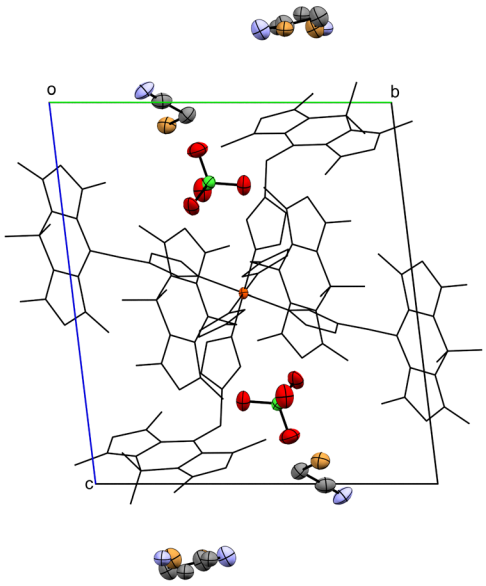

Figure S 9. Structure of coordination compound **2** at 100 K viewed along the crystallographic *a*-axis, showing the relative positions of the solvate molecules ($BrCH_2CN$) and the anion molecules (ClO_4^-) (ellipsoids: 50 % probability level; atom color code: pink…B, grey…C, blue…N, red…O, light green…F, green…Cl, light bronze…Br, orange…Fe; H-atoms are omitted for clarity and **L** molecules are depicted as wireframes for better visualization).

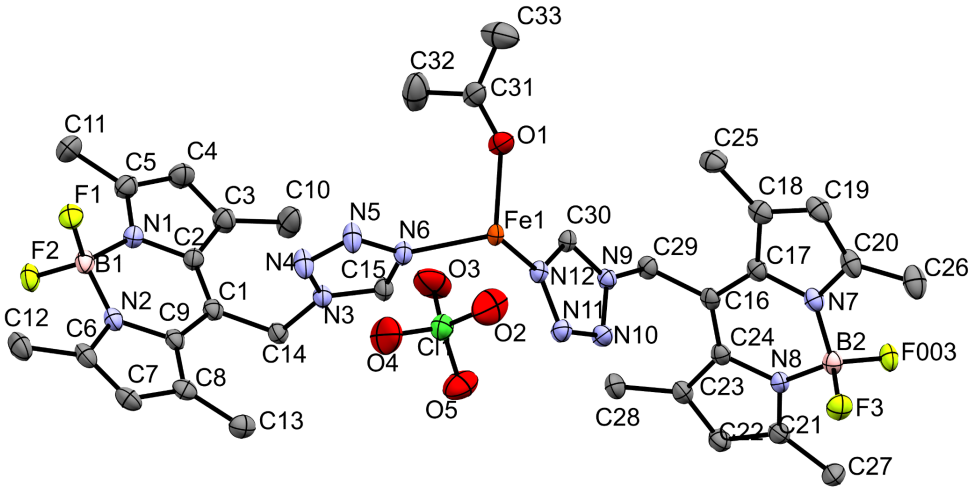

Figure S 10. Asymmetric unit of coordination compound **3** with atomic number labeling, showing the two different conformers of **L** and the co-ligand (acetone) (ellipsoids: 50 % probability level; atom color code: pink…B, grey…C, blue…N, red…O, light green…F green…Cl, orange…Fe; H-atoms are omitted for clarity).

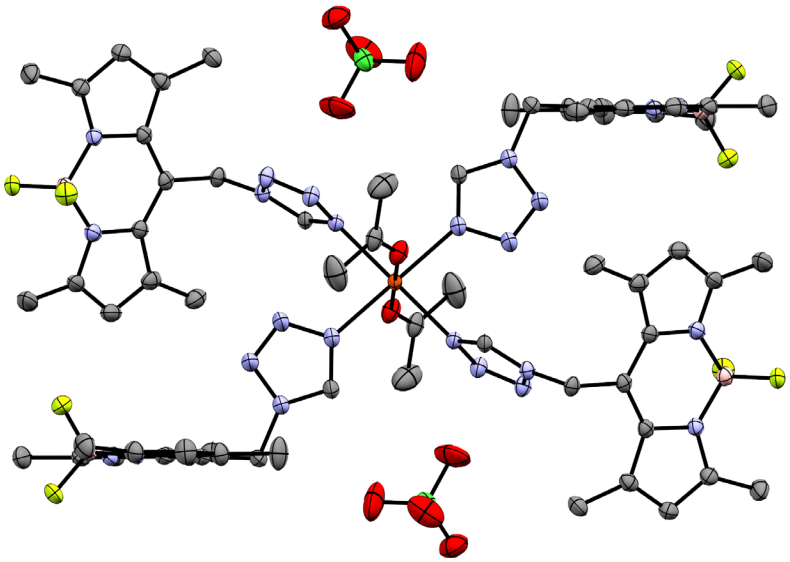

Figure S 11. Structure of coordination compound **3** at 100 K, showing the relative positions of the anion molecules (ClO_4^-) (ellipsoids: 50 % probability level; atom color code: pink…B, grey…C, blue…N, red…O, light green…F, green…Cl, orange…Fe; H-atoms omitted for clarity).

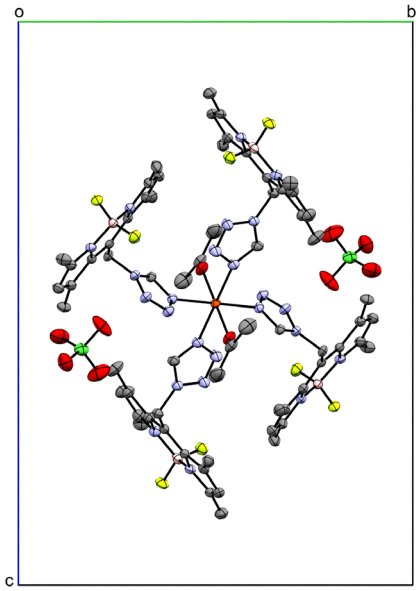

Figure S 12. Structure of coordination compound **3** at 100 K, showing the relative positions of the anion molecules (ClO_4^-), viewed along the crystallographic *a*-axis (ellipsoids: 50 % probability level; atom color code: pink…B, grey…C, blue…N, red…O, light green…F, green…Cl, orange…Fe; H-atoms are omitted for clarity).

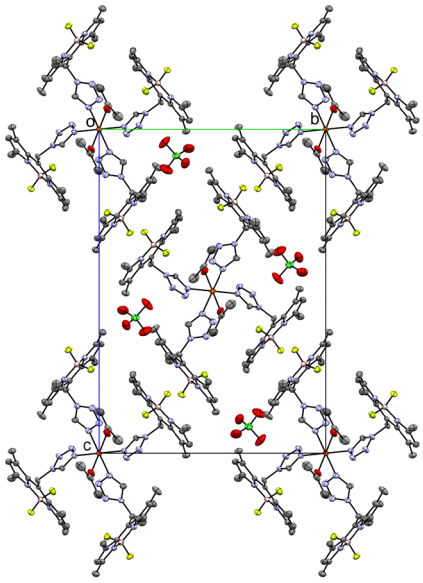

Figure S 13. Crystal packing of coordination compound **3** at 100 K, viewed along the crystallographic *a*-axis (ellipsoids: 50 % probability level; atom color code: pink…B, grey…C, blue…N, red…O, light green…F, green…Cl, orange…Fe; H-atoms are omitted for clarity).

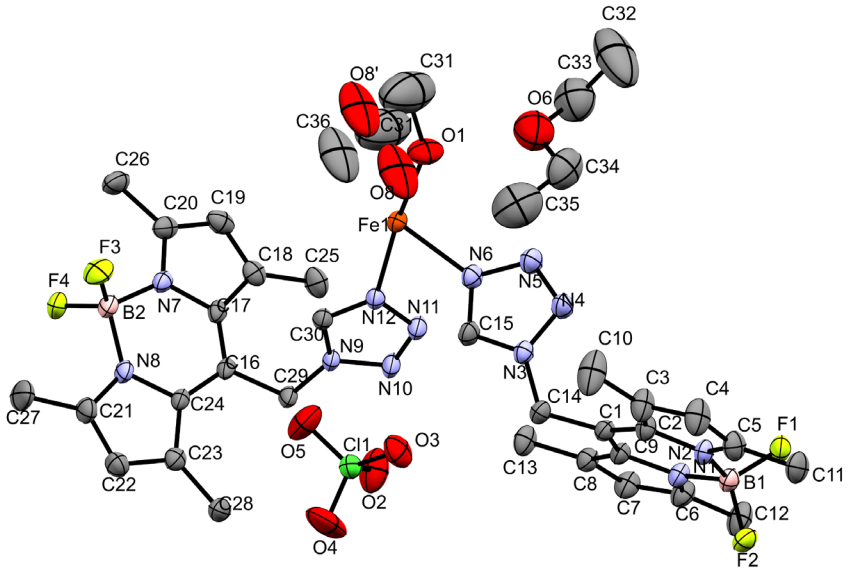

Figure S 14. Asymmetric unit of coordination compound **4a** with atomic number labeling, showing the two different conformers of **L** and the co-ligand (CH_3OH) (ellipsoids: 50 % probability level; atom color code: pink…B, grey…C, blue…N, red…O, light green…F green…Cl, orange…Fe; H-atoms are omitted for clarity).

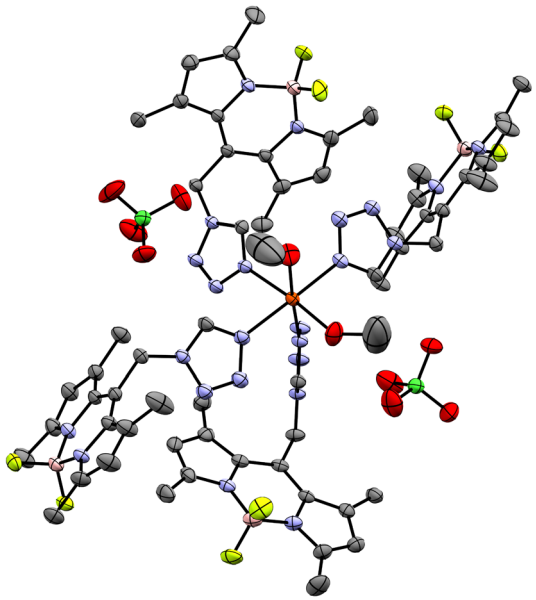

Figure S 15. Structure of coordination compound **4a** at 100 K, showing the relative positions of the anion molecules (ClO_4^-) (ellipsoids: 50 % probability level; atom color code: pink…B, grey…C, blue…N, red…O, light green…F, green…Cl, orange…Fe; H-atoms, solvate molecules and minor positions of the disordered co-ligand are omitted for clarity).

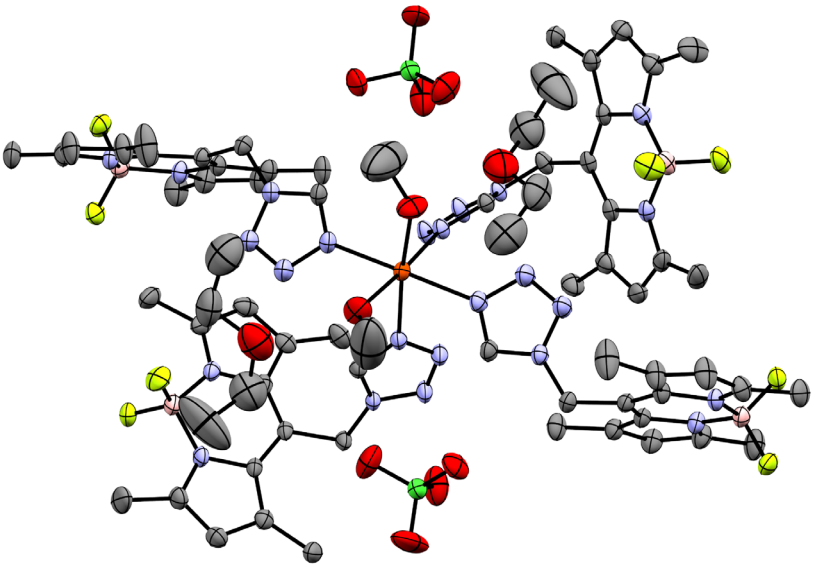

Figure S 16. Structure of coordination compound **4a** at 100 K, showing the relative positions of the anion molecules (ClO_4^-) and the diethyl ether molecules (ellipsoids: 50 % probability level; atom color code: pink…B, grey…C, blue…N, red…O, light green…F, green…Cl, orange…Fe; H-atoms and minor positions of the disordered co-ligand are omitted for clarity).

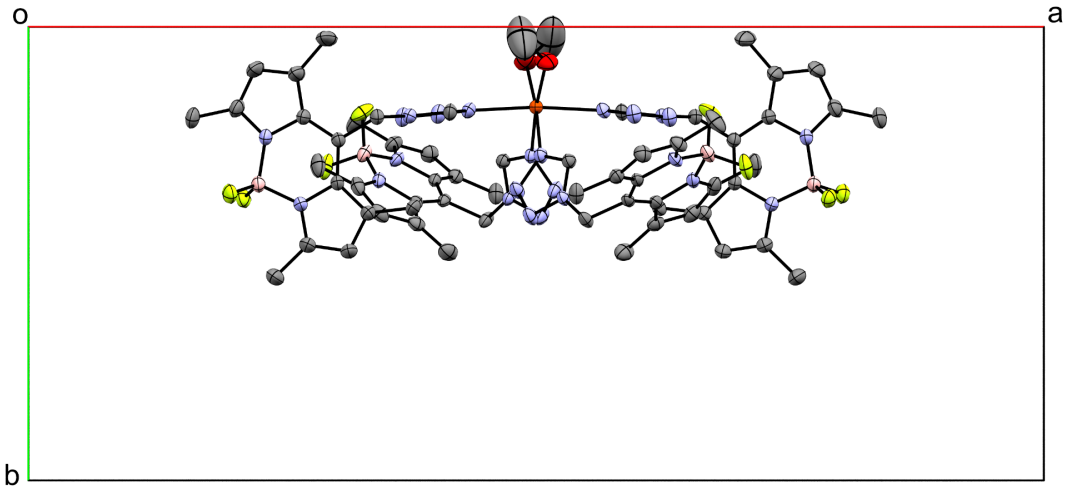

Figure S 17. Molecular structure of coordination compound **4a** at 100 K, viewed along the crystallographic *c*-axis (ellipsoids: 50 % probability level; atom color code: pink…B, grey…C, blue…N, red…O, light green…F, orange…Fe; H-atoms, solvate molecules, non-coordinating anions and minor positions of the disordered co-ligand are omitted for clarity).

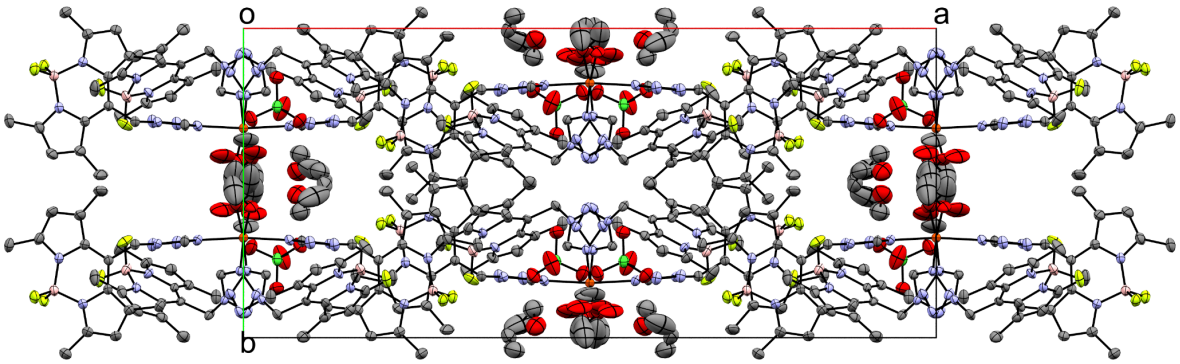

Figure S 18. Crystal packing of coordination compound **4a** at 100 K, viewed along the crystallographic *c*-axis (ellipsoids: 50 % probability level; atom color code: pink…B, grey…C, blue…N, red…O, light green…F, green…Cl, orange…Fe; H-atoms are omitted for clarity).

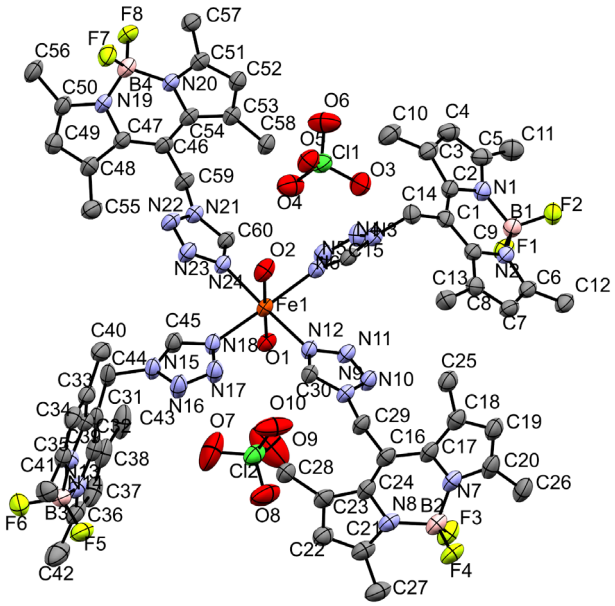

Figure S 19. Asymmetric unit of coordination compound **4b** with atomic number labeling, showing the four different conformers of **L** and the co-ligand (H_2O) (ellipsoids: 50 % probability level; atom color code: pink…B, grey…C, blue…N, red…O, light green…F green…Cl, orange…Fe; H-atoms are omitted for clarity).

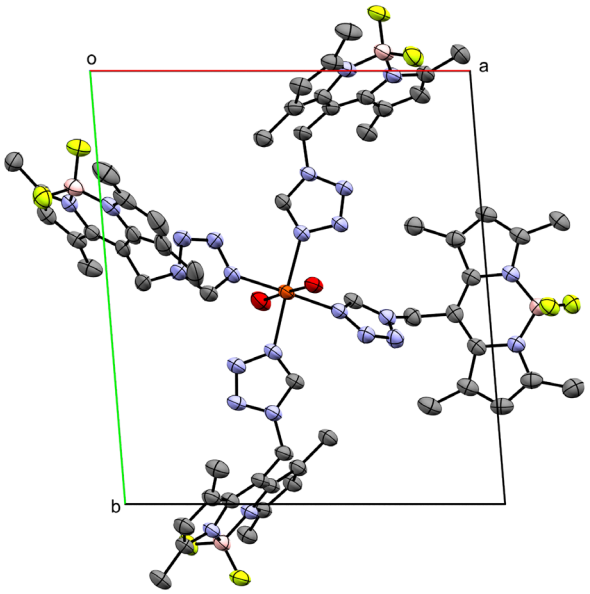

Figure S 20. Molecular structure of coordination compound **4b** at 100 K, viewed along the crystallographic *c*-axis (ellipsoids: 50 % probability level; atom color code: pink…B, grey…C, blue…N, red…O, light green…F, orange…Fe; H-atoms and non-coordinating anions are omitted for clarity).

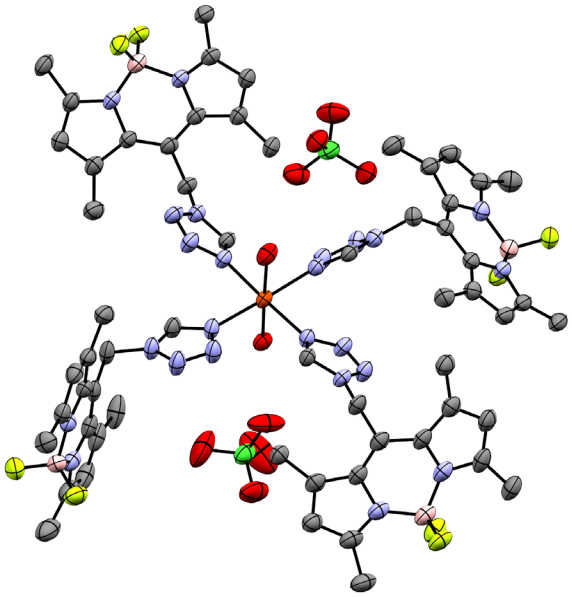

Figure S 21. Structure of coordination compound **4b** at 100 K, showing the relative positions of the anion molecules (ClO_4^-) (ellipsoids: 50 % probability level; atom color code: pink…B, grey…C, blue…N, red…O, light green…F, green…Cl, orange…Fe; H-atoms are omitted for clarity).

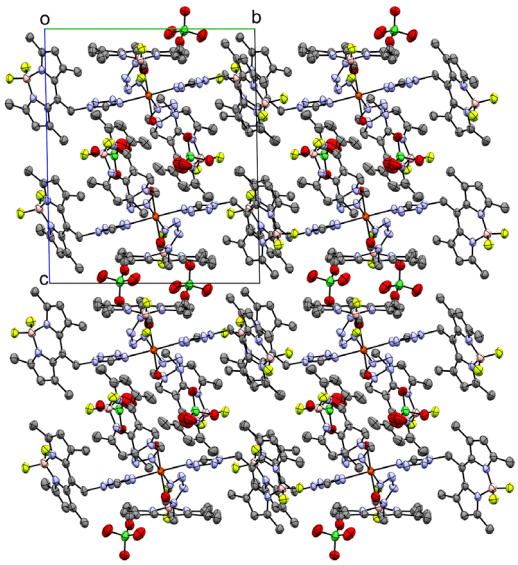

Figure S 22. Crystal packing of coordination compound **4b** at 100 K, viewed along the crystallographic *a*-axis (ellipsoids: 50 % probability level; atom color code: pink…B, grey…C, blue…N, red…O, light green…F, green…Cl, orange…Fe; H-atoms are omitted for clarity).

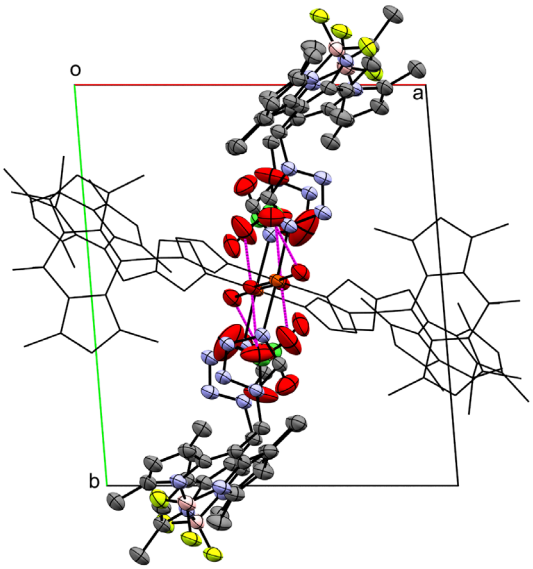

Figure S 23. H-bond network in **4b** at 100 K, forming dimers along the crystallographic *c*-axis (ClO_4^--bridges), which is also the viewing direction and H-bonds represented as magenta-dotted lines (O-O) (ellipsoids: 50 % probability level atom color code: grey…C, blue…N, light green…F, red…O, green…Cl, orange…Fe; H-atoms are omitted for clarity and **L** molecules are partly depicted as wireframes for better visualization).

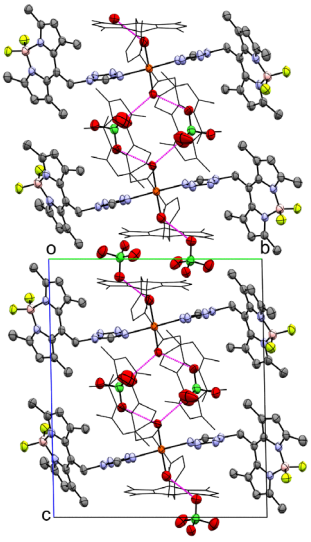

Figure S 24. H-bond network in **4b** at 100 K, forming dimers along the crystallographic *c*-axis (ClO_4^--bridges), viewed along the crystallographic *a*-axis and H-bonds represented as magenta-dotted lines (O-O) (ellipsoids: 50 % probability level atom color code: grey…C, blue…N, light green…F, red…O, green…Cl, orange…Fe; H-atoms are omitted for clarity and **L** molecules are partly depicted as wireframes for better visualization).

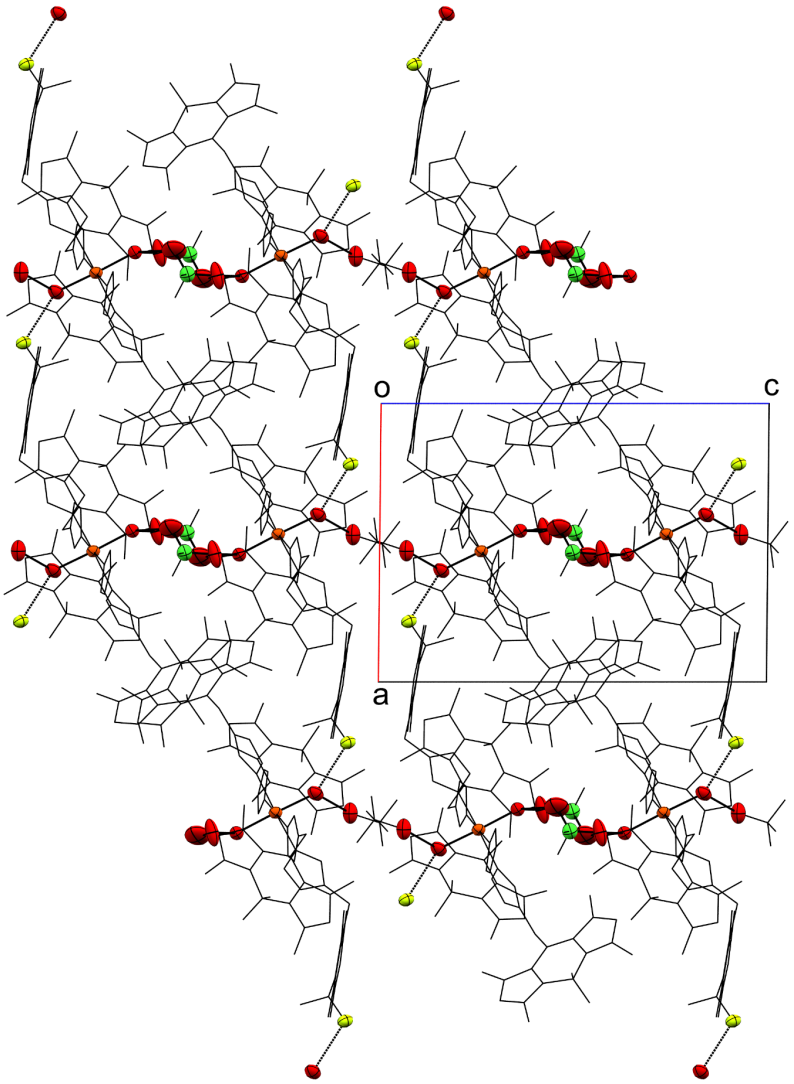

Figure S 25. H-bond network in **4b** at 100 K, forming dimers along the crystallographic *c*-axis (ClO_4^- bridges, O-O) and a one-dimensional periodic network extending along the crystallographic *a*-axis (O-F), with donor/acceptor atom ellipsoids fully shown and H-bonds represented as black-dotted line (ellipsoids: 50 % probability level atom color code: grey…C, blue…N, light green…F, red…O, green…Cl, orange…Fe; H-atoms are omitted for clarity and **L** molecules are depicted as wireframes for better visualization).

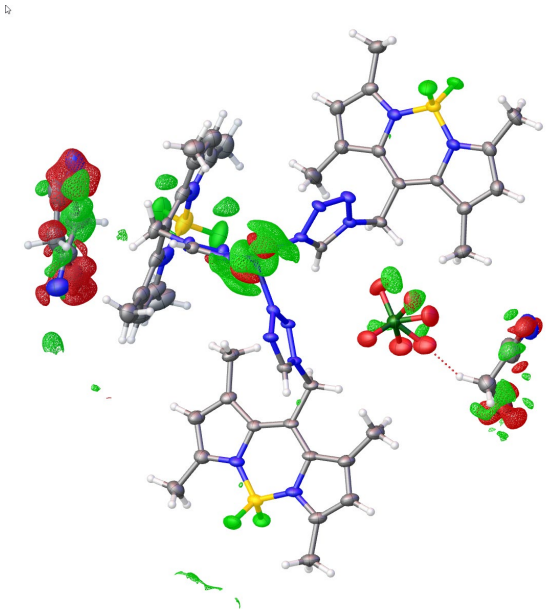

Figure S 26. Difference electron density maps of the crystal structure refinement of **2** showing minor difference electron density around the solvent molecules owing to unresolved disorder.

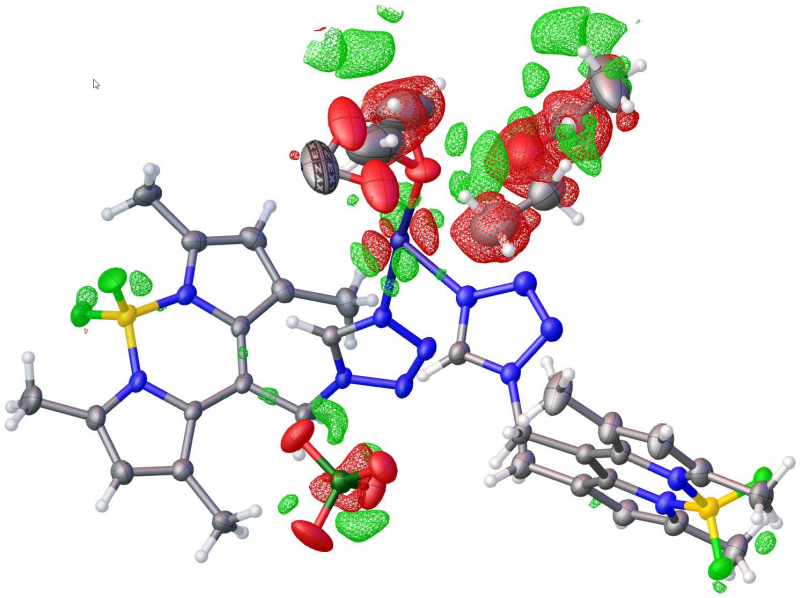

Figure S 27. Difference electron density maps of the crystal structure refinement of **4** showing minor difference electron density around the solvent molecules owing to unresolved disorder.

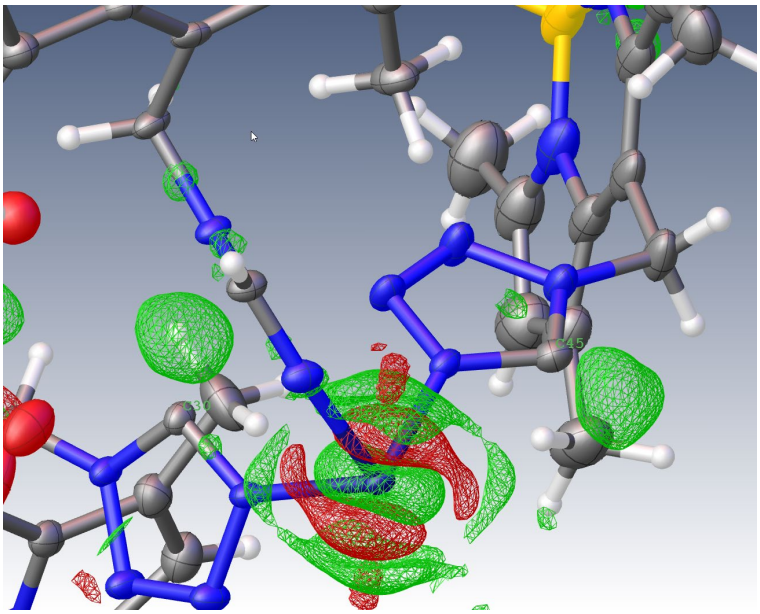

Figure S 28. Difference Fourier maps for **1** (100K), when omitting the H atom from the refinement. Symmetry equivalents are not shown for complexes on a special position.

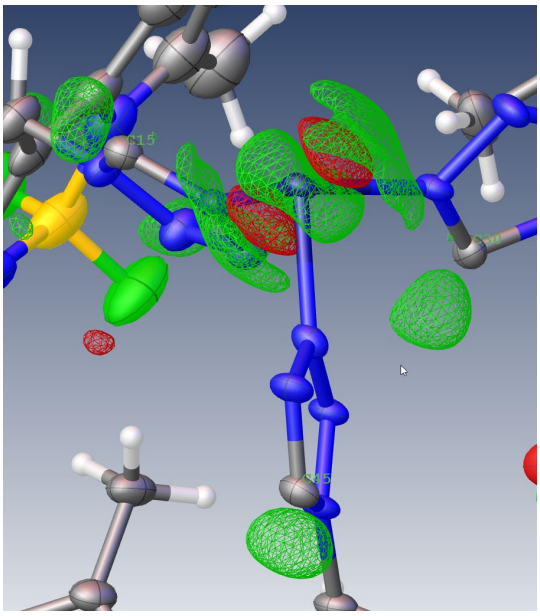

Figure S 29. Difference Fourier maps for **2** when omitting the H atom from the refinement. Symmetry equivalents are not shown for complexes on a special position.

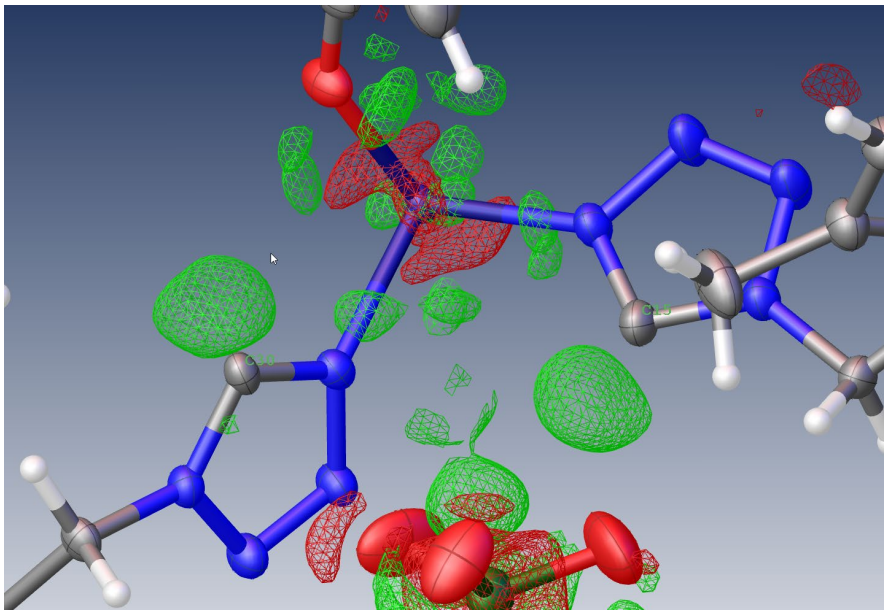

Figure S 30. Difference Fourier maps for **3** when omitting the H atom from the refinement. Symmetry equivalents are not shown for complexes on a special position.

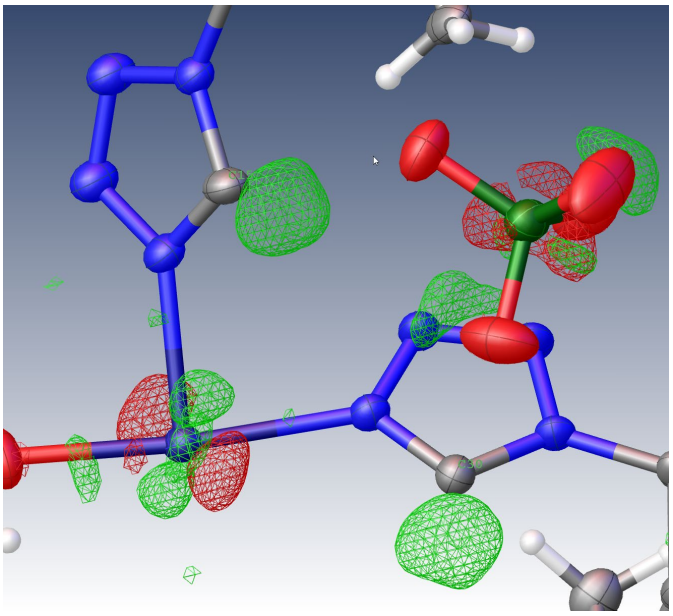

Figure S 31. Difference Fourier maps for **4a** when omitting the H atom from the refinement. Symmetry equivalents are not shown for complexes on a special position.

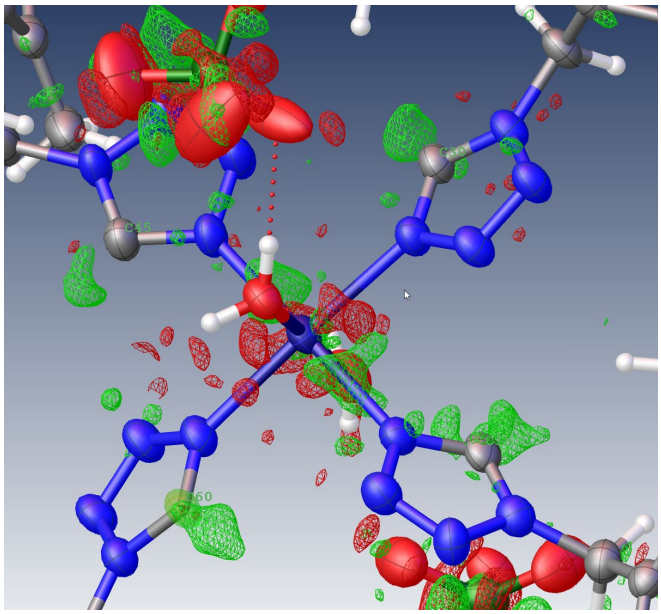

Figure S 32. Difference Fourier maps for **4b** when omitting the H atom from the refinement. Symmetry equivalents are not shown for complexes on a special position.

XRPD measurements

Powder X-ray diffraction experiments were performed on an “Empyrean” (Panalytical) diffractometer using Cu K-α radiation, a primary beam filter (Bragg-Brentano HD), a fixed ½° divergence slit, a 0.04 rad soller slit and a GaliPIX3D detector. Finely powdered bulk samples were positioned on a silicon single crystal cut along the (711) plane. It was measured from 3° to 45° 2 θ with a step size of 0.014°.
Diffractograms were evaluated using the PANalytical program suite HighScorePlus;[2] background correction was applied, and a calculated diffraction pattern derived from single-crystal CIF data was subsequently refined via Rietveld analysis against the measured XRPD data to confirm phase purity and structural consistency.

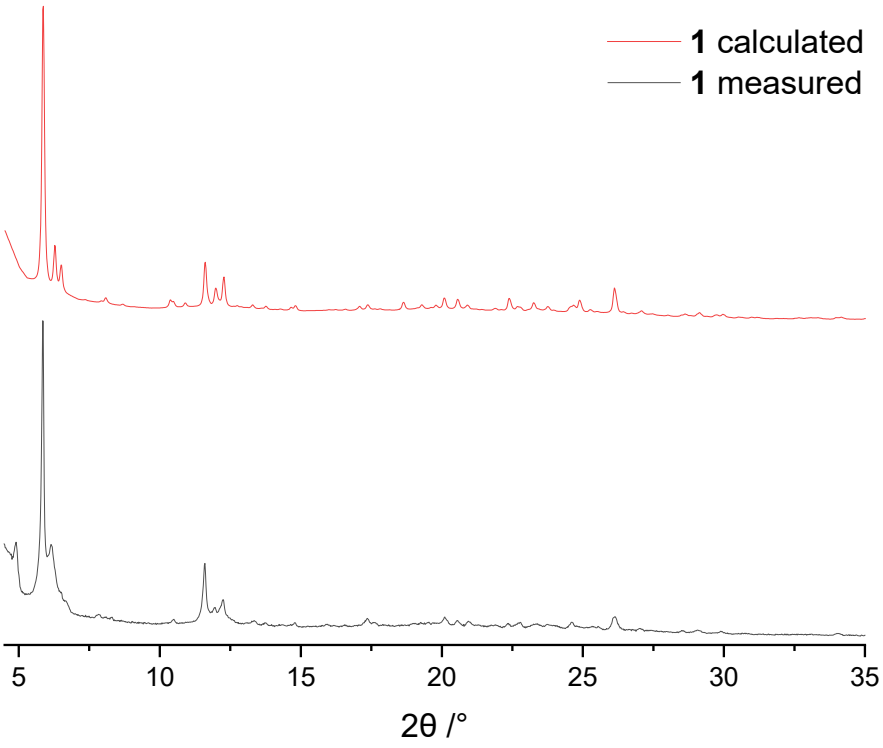

Figure S 33. Experimental XRPD data of **1** (black) compared with the pattern calculated from the single-crystal structure (red).

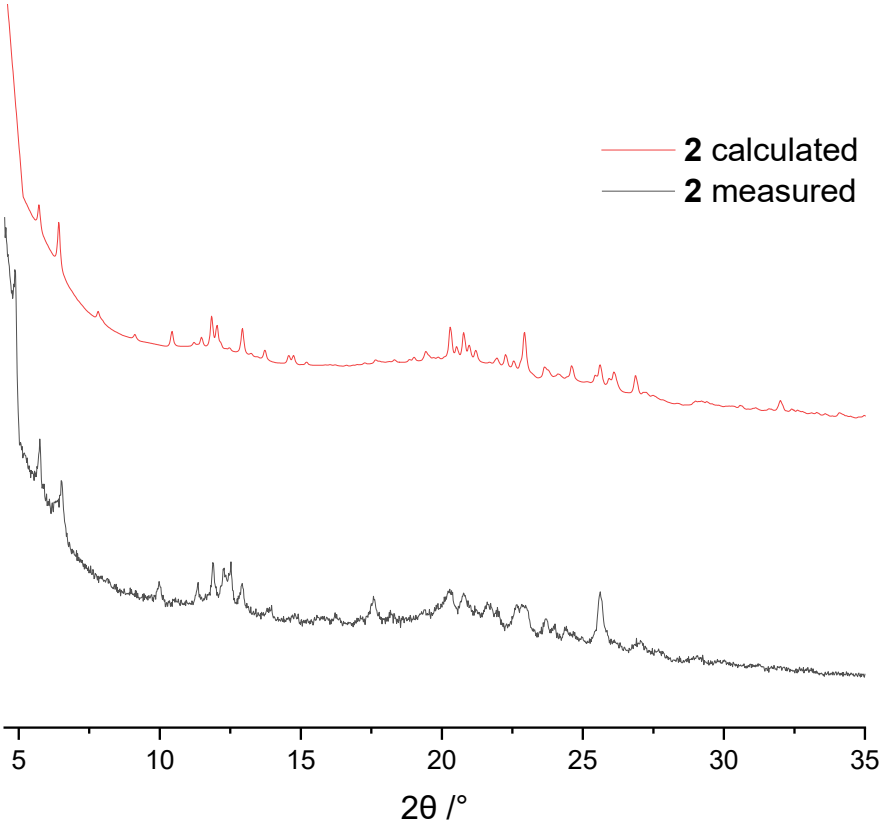

Figure S 34. Experimental XRPD data of **2** (black) compared with the pattern calculated from the single-crystal structure (red).

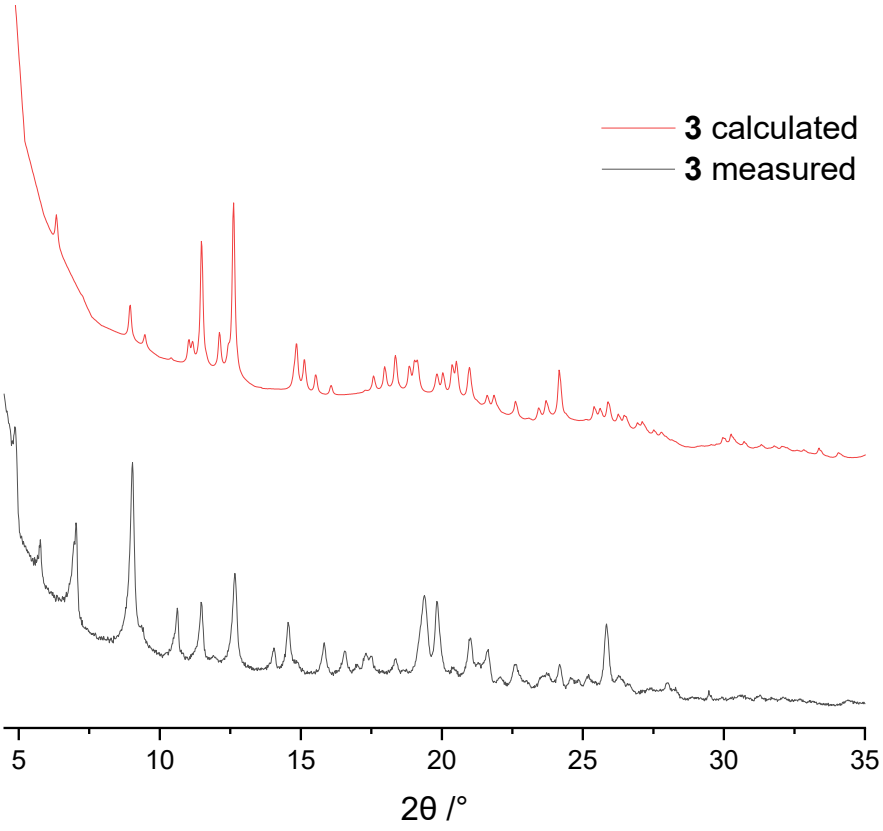

Figure S 35. Experimental XRPD data of **3** (black) compared with the pattern calculated from the single-crystal structure (red).

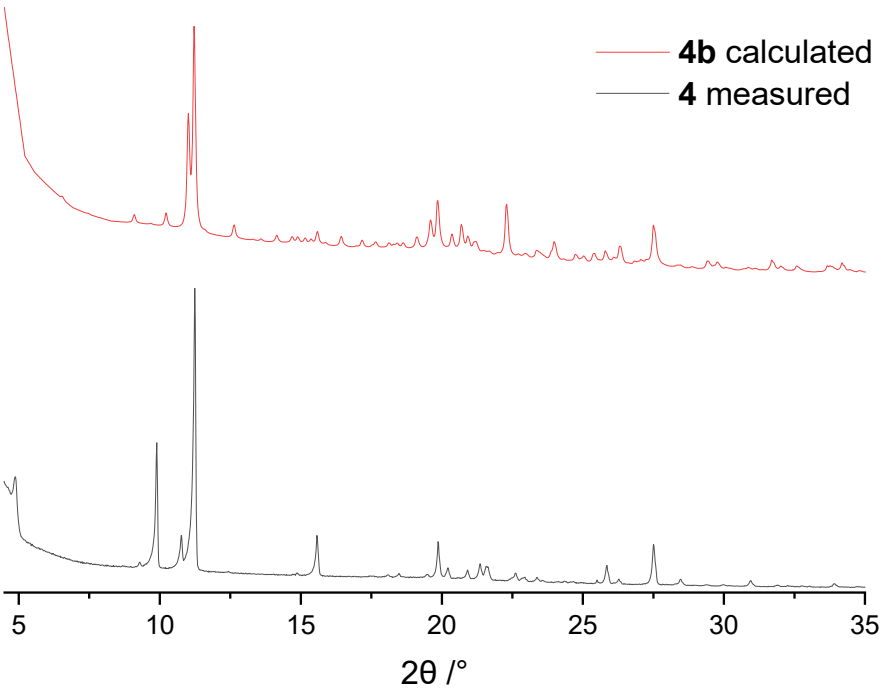

Figure S 36. Experimental XRPD data of **4** (black) compared with the pattern calculated from the single-crystal structure of **4b** (red).

Spectroscopic Measurements

IR spectra were recorded with a SpectrumTwo ATR-FT-IR-spectrometer (Perkin Elmer) using a diamond ATR-unit.

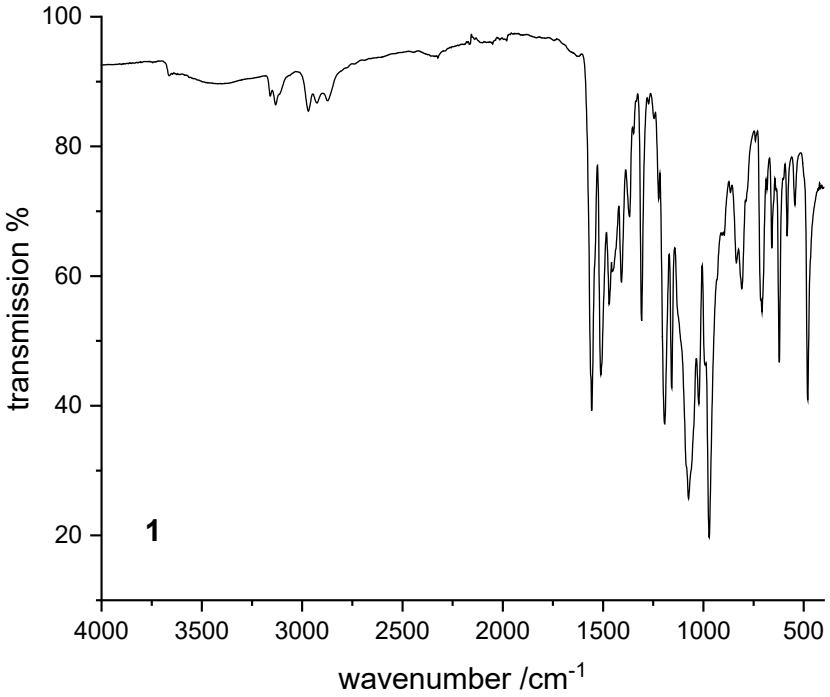

Figure S 37. ATR-IR spectrum of **1** (powder sample).

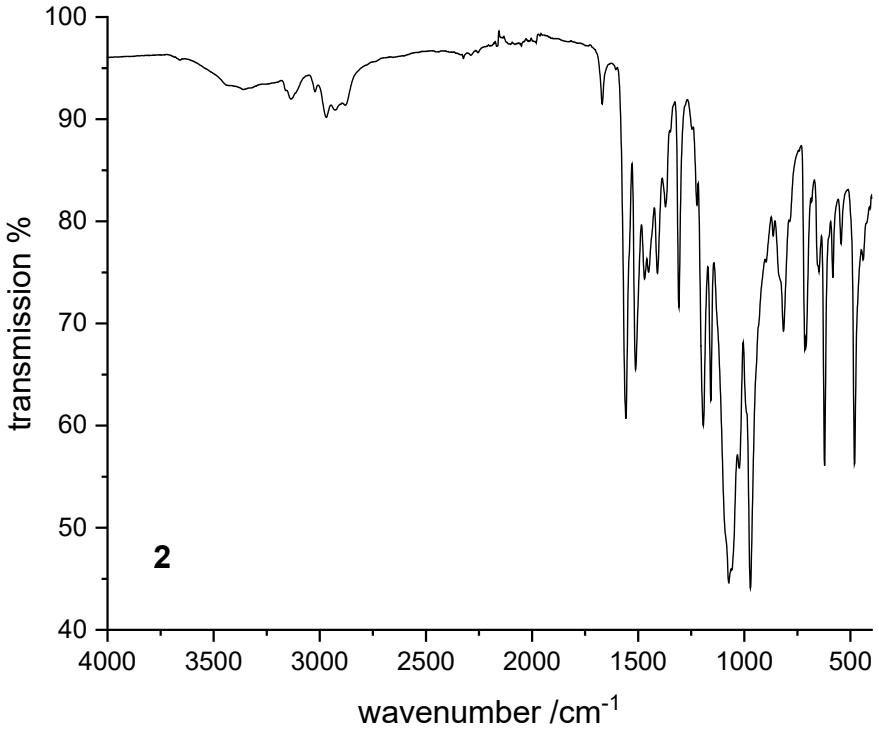

Figure S 38. ATR-IR spectrum of **2** (powder sample).

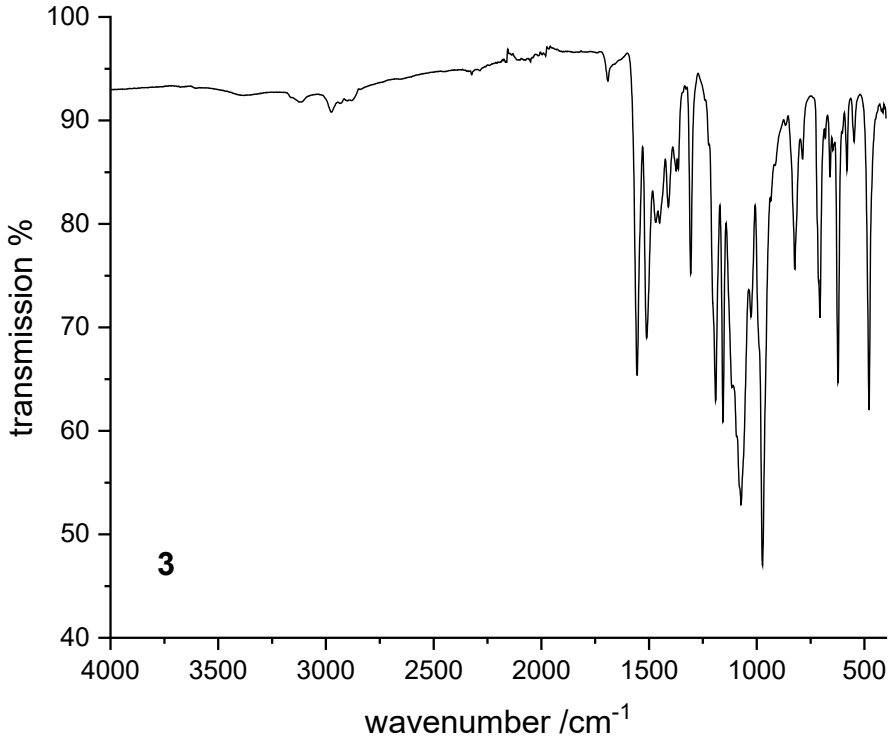

Figure S 39. ATR-IR spectrum of **3** (powder sample).

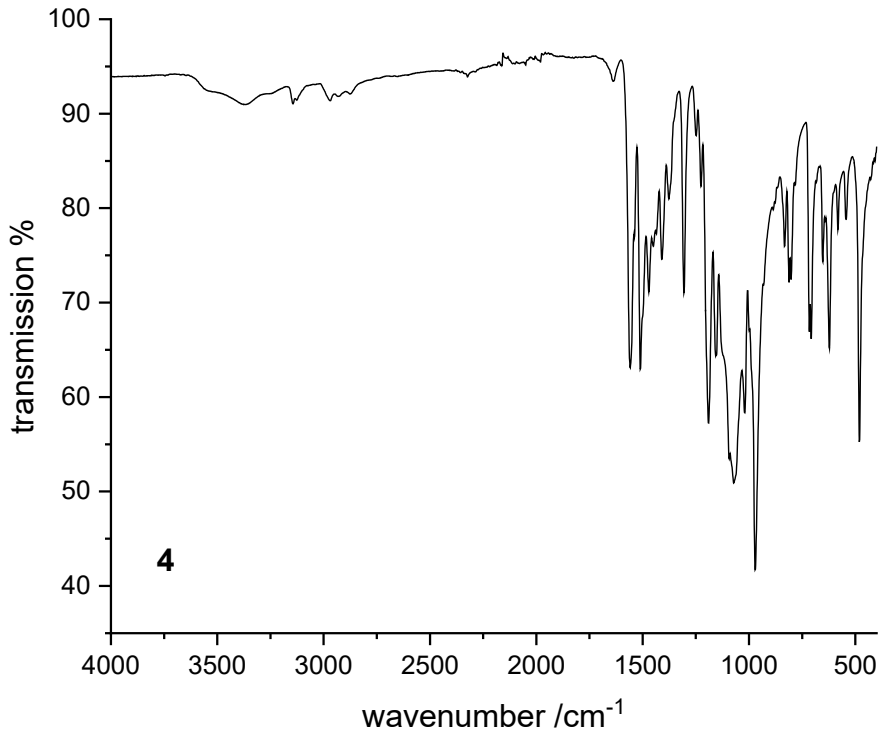

Figure S 40. ATR-IR spectrum of **4** (powder sample).

References

1. M. Huber, M. Schöbinger, J. Cirera, B. Stöger and P. Weinberger, *Eur. J. Org. Chem.*, 2025, **28**, e202401239.
2. T. Degen, M. Sadki, E. Bron, U. König and G. Nénert, *Powder Diffr.*, 2014, **29**, 13-18.
3. G. M. Sheldrick, *Acta Crystallogr. Sect. A: Found. Crystallogr.*, 2015, **71**, 3-8.
4. G. M. Sheldrick, *Acta Crystallogr. Sect. C: Cryst. Struct. Commun.*, 2015, **71**, 3-8.